V-ATPase Deficiency Aggravates Hypoxia-induced Spermatogenesis Reduction by Promoting Spermatocyte Apoptosis via the JNK/c-Jun Pathway in Mice

yin jun (43581886@qq.com)
Third Military Medical University: Army Medical University https://orcid.org/0000-0002-7541-1088

juan Wen He
Third Military Medical University: Army Medical University

Fei Han
Third Military Medical University: Army Medical University

Zhi qi Gao
Third Military Medical University: Army Medical University

Fang Deng
Third Military Medical University: Army Medical University

Wei gong Liao
Third Military Medical University: Army Medical University

Meng jie Zhang
Third Military Medical University: Army Medical University

Qiu Hu
Third Military Medical University: Army Medical University

Zhi fang Li
Third Military Medical University: Army Medical University

Gang Zhang
Third Military Medical University: Army Medical University

Bing Ni
Third Military Medical University: Army Medical University

Research

Keywords: V-ATPase, JNK, c-Jun, DR5, hypoxia, apoptosis, spermatogenesis

Posted Date: March 17th, 2021

DOI: https://doi.org/10.21203/rs.3.rs-300987/v1

Abstract

Spermatocyte apoptosis is the primary cause of poor outcome after hypoxia-triggered spermatogenesis reduction (HSR). The vacuolar H^+-ATPase (V-ATPase) has been found to be involved in the regulation of hypoxia-induced GC-2 cells apoptosis. However, the mechanism of V-ATPase regulating spermatocyte apoptosis after HSR hasnot been well elucidated. In this study, HSRmodel was established by hypoxia exposure in vivo in V-ATPase-knockout (V-ATPase-/-) and wild-type (WT) mice to investigate theeffectof V-ATPase deficiency on spermatocyte apoptosis. GC-2, amouse pachytene spermatocyte-derived cell line, was introduced in vitro experiments. The sperm count and spermatogenic apoptosis were recorded after 60 d of hypoxia exposure in HSR model. The apoptosis of GC-2 cells was detected by flow cytometry and TUNEL staining. The expression of JNK/c-Jun was evaluated by RNA-seq or western blot. The expression of DR_5 and caspase-8 was evaluated by RT-qPCR and western blot. The expression of V-ATPase was determined by western blot in the presence and absence ofLenti-*transcription factor EB* (*TFEB*).C-Jun interference was used for evaluating the role of JNK in regulating the apoptosis of GC-2 cells byTUNEL and flow cytometry. The in vivo results suggested that hypoxia induced spermatogenesis reduction and downregulation of V-ATPase. Moreover, V-ATPase deficiency resulted in moresevere spermatogenesis reduction after hypoxia exposure. The spermatogenesis reduction was associated with exacerbation of spermatocyte apoptosis. Hypoxia down-regulated the transcription of *V-ATPase* through inhibiting *TFEB* and its nuclear translocation. The mRNA and protein expressions of V-ATPaseincreased after *TFEB* overexpression in GC-2 cells. Moreover, V-ATPase deficiency enhanced JNK/c-Jun activation and related DR-apoptotic pathwayin GC-2 cells.However,inhibition of c-Jun attenuated V-ATPase deficiency-induced GC-2 cells apoptosis in vitro and HSR in vivo. In conclusion, JNK/c-Jun was involved in the enhancement of V-ATPase-mediated HSR in V-ATPase -/- mice. V-ATPase deficiency aggravates spermatocyte apoptosis, which may account forthe poor spermatogenesis outcomes of V-ATPase-/- mice. The discoveredfunction of V-ATPase modulating spermatocyte apoptosis indicates its potential therapeutic effect against HSR.

Introduction

Male infertility is a multifactorial pathological problemthat affectsapproximately 7% of the male population[1]. The pathogenesis of these male diseasesis usually attributed tothe below two factors:genetic factors [2, 3] and environmentalfactors. Among the environmental factors, the published literaturesindicated that hypoxia induced-apoptosis of spermatocyte is the central link of male reproductive dysfunction[4, 5]. However, the underlying mechanism of hypoxia induced-apoptosis of spermatocyte remains largely unclear.

Transcription factor EB (TFEB), a member of the bHLH transcriptionfactor TFEB-MITF family, is a master regulator of lysosome biogenesis and autophagy-related gene transcription [6, 7]. Starvationregulates the biogenesis of V-ATPase subunits by decreasing mTORC1activity, which subsequently facilitates the entry of the TFEB into the nucleus andthen induces a series of V-ATPases transcription[8].

The vacuolar H^+ (V)-ATPase (V-ATPase) is a macromolecular complex, which is responsible for pumping protons (H^+) into lysosomes and lowering intraluminal pH to the acidic range. V-ATPaseneedsto activate dozens of hydrolases with acidic pH optima in lysosomes, thereby controlling several events in the secretory and endocytic pathway, such as autophagy [9]. Deletion of V-ATPase in cardiomyocytes, hepatocytes or podocytes may lead to a significant decrease of V0 subunits and autophagy defects[10–12]. In addition, when amino acids are scarce, V-ATPase would be more active to obtain the increased capacity for rapid re-acidification afterautophagosome-lysosome fusion, thusacceleratingdigestion rate and protein circulationby lysosome[13].This process occurs via amino acid-regulated associations among the V-ATPase, Rag-GTPases and Ragulator, ultimately allowing the V-ATPase to promote lysosomal function, and V-ATPase is considered as a signaling molecule for nutrient sensing [14, 15]. It was reportedthat inhibition of V-ATPase blocked autophagic flow and caused accumulation of autophagosomes, which could be inhibitedby mTORC1[16]. Interestingly, it was also reported that mTORC1 signaling could be inhibitedby V-ATPase, and the main manifestations of V-ATPase mutant mice is decreased autolysosome degradation[16]. Therefore, V-ATPase represents a prime target that may promote autophagic degradation[17].

Autophagy can attenuate cell death by selectively reducing the abundance of pro-apoptotic proteins in the cytosol. Colon cancer cells lacking the pro-apoptotic protein BAX are resistant to TRAIL (TNF-related apoptosis-inducing ligand)-induced cell death unless autophagy is inhibited. In which, autophagy mediates the selective removal of active caspase 8[18]. Similarly, in a model of tumor necrosis factor (TNF)-induced hepatocyte apoptosis, inhibition of autophagy by liver-specific knockout of Atg7 increased caspase 8 activity[19]. In line with this observation, in our previous study, we found that hypobaric hypoxia inhibited the autophagic degradation, as well as the expression of V-ATPase[20]. Moreover, the activation of V-ATPase and autophagy caused by overexpression of Beclin-1 reduced the apoptosis of spermatocytes[20]. This evidence indicates that spermatocyte apoptosis induced by hypoxia might correlate with V-ATPase. However, the underlying mechanisms are still unclear and need to be clarified further.

The c-Jun N-terminal kinase (JNK), also known as a stress-activatedprotein kinase (SAPK) of the MAPK family, is initially activated inresponse to a variety of stress signals, and has been implicatedin many cellular events including apoptosis and autophagy[21–24]. Overwhelming evidences have unequivocally unraveled the roleof the JNK in cancer cells apoptosis, and its repression has been traditionallyassociated with a resistant phenotype to various genotoxicstimuli, such as chemotherapeutic drugs[25–27]. However, the relationship between JNK and apoptosis in non-cancer cells, especially in spermatocytes is not clear. Therefore, considering the effect of V-ATPase on spermatocyte apoptosis and JNK as a key mediator of hypoxia-induced apoptosis, this study investigated the underlying mechanism of V-ATPase inhibiting spermatocyte apoptosis in vivo and in vitro.

Materials And Methods

Cell culture, hypoxia treatment and transfection

Mouse pachytene spermatocyte-derived cell line GC-2 were obtained fromZhong Yuan biological Ltd (Beijing, China) and were cultured in DMEM as described previously[28]. Where indicated, hypoxia (1% O_2) was achieved by a mixture of ultra-high purity gases (5% CO_2, 10% H_2 and 85% N_2)ina 37^oChypoxia workstation (Invivo$_2$, Baker Ruskinn, Sanford, ME, USA). All experimentaloperations including RNA and protein isolation were performed in the hypoxia workstation.

The hypoxic model of GC-2 cells was established according to thetreatment of different time. For different time treatment, 5×10^5 cells/well were implanted at six well dish (diameter 35mm) in a 37^oC, 21% O_2 and 5% CO_2 incubator. The cells were washed once with phosphate buffer saline (PBS) after 24 h and then the cells were cultured in a 37^oC, 1% O_2hypoxia workstation for 24 h.

Small interfering RNA sequences for mouse V-ATPase were as follows: *GCCCUUGGAAUGUCUAAUATT* (sense) and *UAUUAGACAUUCCAAGGGCTT* (antisense). Small interfering RNA sequences for mouse HIF-1α were as follows:*GGGCCAUAUUCAUGUCUAUUU*(sense) and *AUAGACAUGAAUAUGGCCCUU*(antisense). Small interfering RNA sequences for negative control were as follows: *UUCUCCGAACGUGUCACGUTT* (sense) and *ACGUGACACGUUCGGAGAATT* (antisense). Transient transfections were performed with Lipofectamine 3000 (Invitrogen, California, USA). Experiments were routinely performed in triplicate wells and repeated three times.The mouse V-ATPase cDNA (Open Biosystems) was PCR amplified and cloned into the third-generation self-inactivating lentivirus (LV) vector.The expression was driven by cytomegalovirus (CMV) promoter, andthe vector LV-V-ATPase was constructed[29]. Lentiviruses expressing V-ATPase or empty vector (as controls) were prepared by transient transfection in 293T cells[30]. For all experiments, cells were infected with LVs expressing V-ATPase at a multiplicity of infection (MOI) of 10. For TFEB overexpression, the coding regions of TFEB wereamplified from rat cDNA by real-time quantitative reversetranscription polymerase chain reaction (RT-qPCR) andwere cloned into the GV492 plasmids. The final recombinant GV492-TFEB-overexpression expression cassette was LTR-Ubi-TFEB – 3FLAG -CBh -gcGFP-IRES-puromycin-LTR.The vector was confirmed by sequencing.The resultant AAVs were packaged at Gene ChemBiotechnologyCompany (Genechem, Shanghai, China). The packaged GV492 were concentrated in phosphate-buffered saline (PBS; HyClone,sh30256.01) at the following titers: GV492-TFEB-overexpression (Lenti-TFEB, 3×10^8TU)and GV492-TFEB-negative control (Lenti-NC, 5×10^8TU)genome copies per milliliter.After infection with 10 MOI, cells were incubated in a humidified, 5% CO_2 atmosphere at 37°C. All experiments were conducted in triplicate to ensure reproducibility.

Mice

All protocols were approved by the Third Military Medical University Institutional Animal Care and Use Committee and conducted following the National Institutes of Health guide for the care and use of laboratory animals (*NIH Publi*cations No. 8023, revised in 1978). The V-ATPase KO mice were purchased from Nanfang Model Organisms Center, Shanghai, China. Hypoxic mice were raised in a hypobaric

chamber, where the atmospheric pressure was reduced to simulate an altitude of 6000 m. The partial pressure of nitrogen falls as total pressure declines on ascent, but the nitrogen percentage in the atmosphere does not change. Hypoxic mice were returned to normobaric conditions for 40 min every day. Control mice were raised at an altitude of 300 m out of the hypobaric chamber. All the animals had free access to standard pellet food and water, and they were maintained under controlled lighting conditions (12 h light:12 h darkness), ambient temperature maintained at 22-24^{o}C, and relative humidity of 40–60%. At day 1, LV-V-ATPase mice were injected with100μLof the lentiviral preparations (5 × 10^{8}TU/mL) into the testicular tissue.

Epididymal sperm count

Mice were sacrificed by an overdose of anesthesia.The epididymis was removed and weighed when dry. Then, they were divided into two parts, head-body and cauda. The method described by Vega *et al*. was used for sperm count of epididymis cauda[31]. In brief, Caudal regions from the epididymis were isolated and minced. Sperm cells were allowed to disperse out of the cauda. Sperm suspensions were prepared by mincing cauda in 2 mLof phosphate-buffered physiological saline (PBS, pH = 7.2). The suspension was pipetted and filtered through 80 μm nylon mesh to remove tissue fragments. An aliquot (0.05 mL) from the sperm suspension (1 mL) was diluted with 1:50 PBS (PBS, pH 7.2) and mixed thoroughly. An aliquot of the mixture (50 μL) was analyzed for sperm concentration and progressive motility using a Sperm Class Analyzer (Microptic S.L., Barcelona, Spain). The sperm concentration per μLwas multiplied by 50 to obtain total sperm count.

Haematoxylin and eosin (HE) staining

Animals were euthanizedby decapitation. The left testis was excised, fixed in 10% formalin, dehydrated, and embedded in paraffin. Sections were cut at 5 μm thickness and were stained with HEfor light-microscopic observations.

TUNEL assay

Paraffin-embedded sections were cut into thin slices (4 μm) and deparaffinized. Nuclei were processed according to the manufacturer's instructions of a TUNEL assay kit (Beyotime). Briefly, the sections were permeabilized with 0.1% Triton X-100,followed with fluorescein isothiocyanate (FITC)-labeled TUNEL staining for 1 h at 37^{o}C. Nuclei were then counterstained with DAPI. The total number of TUNEL-positive nuclei and spermatogenic cells were counted under laser scanning confocal microscope (IX81, Olympus, Tokyo, Japan) and quantified as the number of green spots in each photograph (×200) with the assistance of ImageProPlus software.10 photographs were counted.

RNA-seq

After being treated with hypoxia (1% oxygen concentration) or normoxia(21% oxygen concentration) control for 48 h, GC-2 cells were collected and total RNA was extracted using TRIzol reagent (Invitrogen, Carlsbad, CA,USA). RNA-seq analysis was performed by Personalbio Genomic Technology Co Ltd (Shanghai, China)[32]. Briefly, total mRNA was extracted by a Dynabeads mRNA DIRECT Kit (Ambion).

Thereafter, the cDNA library was constructed using NEBNext Ultra TM Directional RNA Library Prep Kit for Illumina (New England BioLabs Inc.). After fragmentation and conjugation with sequencing adapters, the cDNA libraries were sequenced on Illumina Hiseq 2500 platform using PE100 strategy. The raw data from RNA-seq were filtered and mapped to a reference genome (Mus_musculus.GRCm38.90. chr) by using FASTX. The FPKM (fragments per kilobase of exon model per million reads mapped) was calculated from the filtered and mapped clean raw reads. Furthermore, we employed the tximport package with default parameters to remove abnormal low-/high-abundance transcripts from the transcriptomic profiles. Eventually, the DEGs were obtained from DESeq2 analysis and used for further bioinformatics study.The raw data are accessible toBioProject PRJNA608077 with SRA accession number SRP256125 (experiments SRR11534018-SRR11534023). The raw data set and expression values used for surprisal analysis are made public to enable critical or extended analyses.

Bioinformatics analysis

The sequencing results were processed and the clean reads from the RNA-seq libraries were mapped to the mouse reference genome (Mus_musculus.GRCm38.90. chr) with HISAT2 v2.1.0. Differential expression analysis of six samples was performed using DESeq2. We identified differentially expressed genes (DEGs), based on the criteria that $P < 0.05$ and |log2 (fold change) | > 1.5. The *P*-values were adjusted using the Benjamini and Hochberg method. The volcano plot of DEGs and cluster diagrams were prepared by R packages “ggplots” and “ggplot2,” respectively. KEGG pathway was based on the Kyoto Encyclopedia of Genes and Genomes database, and it was performed to explore the pathways related to these DEGs[33]. A *P* value of less than 0.05 was considered as statistically significant. The enrichment ratio of these pathways was ranked based on the normalized enrich scores (NES). The coefficient r in each gene set was calculated by the Pearson correlation.

Western blotting

After hypoxia treatment, total protein was extracted using a Western & IP cell lysis kit (Beyotime)containing1mM PMSF. Nuclear and cytoplasmic proteins were separated using the Nuclear and Cytoplasmic Protein Extraction Kit (Beyotime) according to the manufacturer’s instructions.Whole cell extracts were then separated by 10% sodium dodecylsulfate–polyacrylamide gel electrophoresis and electrotransferred to a polyvinylidenedifloride (PVDF) membrane (Beyotime). Afterblocking, the membranes were incubated at $4^{o}C$ overnight with rabbit polyclonal Antibodies against Vacuolar H^{+} ATPase (VMA21/V-ATPase, 1:1000 dilution,ab242099, Abcam, Cambridge, UK), TUBB1/β-tubulin (1:1000 dilution, Sigma,T7816), laminB(1:1000 dilution, Sigma, SAB1306342), TFEB(1:1000 dilution, SAB2107961, Sigma), $LAMP_2$(1:1000 dilution, AF1036, Beyotime), JNK1 (1:1000 dilution, 3708, CST), Phospho-JNK1 (1:1000 dilution, 9255, CST), c-Jun (1:1000 dilution, 9165, CST), Phospho-c-Jun(1:1000 dilution, 9261, CST), DR_5 (1:500 dilution, ab8416,Abcam, Cambridge, UK),Caspase-8 (1:1000 dilution, 4790, CST) and β-actin(1:1000 dilution, sc-8432, Santa Cruz), Then the membranes were washed with TBST and incubated with horseradish peroxidase-linked secondary antibodies (ZDR-5306, ZDR-5307,Zhong Shan, Beijing, China). After being washed with TBST, immunoreactive bands were visualized using NBT/BCIP (Beyotime)as substrate.

Apoptosis detection by flow cytometry

Apoptotic incidence was measured with the AnnexinV-FITC apoptosis detection kit I (Beyotime, Nanjing, China) according to the manufacturer's instructions. Briefly, cells were washed twice with cold PBS, and then resuspended in 200 μLof binding buffer at a concentration of 1×10^6 cells per mL. 2μLof annexin V-FITC solution and 10μLof PI (propidium iodide) were added to these cells at 37°C for 30 min. The cells were analyzed by flow cytometry (FACSCalibur; BD Biosciences, San Diego, USA)within 1 h. Apoptotic cells were counted and represented as a percentage of the total cell count.

RNA isolation and real-time polymerase chain reaction

Total RNA was extracted from treated cells using 1 mL TRIZOL reagent (TaKaRa Bio, Shiga, Japan). cDNA was synthesized from 1μg total RNA through reverse transcription using a TaKaRa RNA PCR Kit (TaKaRa Bio). The sequences for primers are shown as following: V-ATPase (forward,5'-*CACAGAGATGTCCCTTGATGT*-3' andreverse,5'-*GTTGTGATGACGCAGCTTT*-3'); TFEB (forward,5'-*AAGAACAGGGGTGAGGCA*-3'andreverse,5'-*CCCAGGCTCAGGAGAGG*-3'); c-Jun(forward,5'-*GGGTGCCAACTCATGCT*-3' andreverse,5'-*CTCTGTCGCAACCAGTCAA*-3'); JNK1(forward,5'-*GCGTCCCATCTTTTAGTGA*-3' andreverse,5'-*TCATGCTCCAATTTCTGCT*-3'); DR5(forward,5'-*CAGCCCAACCAGAGACA*-3' andreverse,5'-*AGAGCCTGCATCTTCGG*-3') ; Atcb(forward,5'-*CCTCACTGTCCACCTTCC*-3' andreverse,5'-*GGGTGTAAAACGCAGCTC*-3'). Quantitative real-time PCR was performed by using 1μg of cDNA and SYBR Green (BioRad, California, USA) in 96-well plates in a LightCycler rapid thermalcycler system (MJ research, Therma). PCR products were subjected to melting curve analysis, and the data were analyzed by the $2^{-\Delta\Delta CT}$ calculation method and standardized by β-actin.

Immunofluorescent staining

Sterilized coverslips were placed in 24-well plates during GC-2 cell plating.Then, cells were washed three times with wash buffer (Immunol Fluorence Staining Kit, Beyotime). Nonspecific binding sites were blocked for 60 min at room temperature with confining liquid. Then, without further washing, cells were incubated with aTFEB Rabbit Polyclonal Antibody(1:200 dilution, AF8130, Beyotime) for 60 min at room temperature. TFEB staining was revealed by incubation with Alexa Fluor™ 488 donkey anti-rabbit IgG(H + L) (1:500 dilution, A21206, Invitrogen) for 60 min at room temperature. Cell nuclei were stained with DAPI (C1005, Beyotime) for 5 min at room temperature. Then, the cells were observed under laser scanning confocal microscope (IX81, Olympus, Tokyo, Japan) in random microscopic fields at ×400 magnification.

Statistical analysis

All data were expressed as mean ± standard deviation (SD). Statistical analyses were performed using the SPSS 20.0 statistical software program. Statistical significance was evaluated by one-way analysis of variance (ANOVA), followed by the least significant difference (LSD) test.

Results

1. Hypoxia down-regulated testis V-ATPase and induced spermatogenesis reduction in mice

In our previous studies, we demonstrated that hypoxia cut off the autophagic flux of GC-2 cells in vitro by inhibiting V-ATPase; activation of autophagy can significantly rescue hypoxic spermatogenesis reduction (HSR) [20]. In this study, we observed that the mice exposed to hypoxia showed a considerable increase inapoptosis of spermatogenic cells (Figure S1A). The apoptosis analysis of spermatogeniccells in seminiferoustubules by confocal microscopy showed a11-fold of apoptosisincrease in mice exposed to hypoxia for 15 din compared with the control(Figure S1B).Significantly decreased sperm count was also observedafter 15 days of hypoxia exposure (Fig. 1A). Meanwhile, hypoxia significantly increased the protein level of DR_5(Death Receptor 5, a key molecule of death receptor apoptosis pathway) and decreased V-ATPase expression in mice (Fig. 1B). These data indicated that hypoxic exposure can triggerspermatogenesis reduction and bring about DR5 increase and V-ATPase reduction.

2. Overexpression of V-ATPaseimprovedspermatogenesis by inhibiting apoptosis of spermatogenic cells in hypoxic mice

Subsequently, we exploredwhether overexpression V-ATPase affected spermatogenesis under different hypoxic exposure conditions. V-ATPase KO mice was used as the positive control to further examinethe pathological damage of seminiferous tubules in LV-V-ATPase mice under different hypoxic condition. The results showed that the damage degree of seminiferous tubules in LV-V-ATPase mice was further alleviated, including the decrease of spermatogenic epithelial exfoliation and spermatogenic cell apoptosis. In contrast, V-ATPase-KO mice showed a considerable increase inapoptosis of spermatogenic cells (Figure S2A). TUNEL assay indicated that the apoptotic rate of spermatogenic cells was remarkedly reduced after lentivirus treatment(Figure S2B). Moreover,sperm count was significantly increased in LV-V-ATPase group compared with the other groups(Fig. 2A). In addition, overexpression of V-ATPase by lentivirus resulted in marked reduction of DR5 levels and caspase-8 protein expression in mice under hypoxia exposure (Fig. 2B), indicating that V-ATPase may be involved in regulating the apoptosis of spermatogenic cells under hypoxia.However, it is not clear which type of spermatogenic cells apoptosis is regulated by V-ATPase.

3. Hypoxia down-regulated V-ATPase through inhibiting TFEB transcription and nuclear translocation in GC-2 cells

Previous reports have indicated that spermatocytes are most sensitive to hypoxia in spermatogenic cells[4]. Herein, our further experiments were conducted to determine the effect of different hypoxia time on the apoptosis of GC-2 cells by measuring the apoptotic rate at 0h, 24h and 48h after exposure at 1%

O_2. The morphology of hypoxia-treated cells was evaluated under a laser scanning confocal microscope.The results showed that there was no difference in the percent of apoptotic cells between 0h treatment group and 24h treatment group after exposure at 1% O_2. However, a significant increase inchromatin condensation and nuclear fragmentationoccurred in the GC-2 cells after 24h of hypoxia treatment (Figure S3A), reflecting the inducing effect of hypoxica on the apoptosis of GC-2 cells. The FCM assay further confirmed this observation (Figure S3B). Furthermore, western blot results showed that hypoxia induced an increase in the protein levels of DR_5, Caspase-8, as well as a decrease in the mRNA and protein levels of V-ATPase (Figure S3C andS3D). These results together indicated that hypoxia inhibitsV-ATPase expression and causes spermatogenesis reduction, which is associated with extrinsic apoptosis pathway of spermatocyte.

It is well known that TFEB homologues induce the transcription of several *V-ATPases* in *Drosophila* and mammals[8, 34].Therefore, it is necessary to further study whether TFEB is involved in hypoxia-induced inhibition of V-ATPase expression.Therelative abundance of endogenous TFEB in total, nuclear andcytoplasmic fractions of GC-2 cells was firstly examined. Thedata showed that in total extracts of hypoxia-treated GC-2 cells, the mRNA and protein levels of TFEB were significantly down-regulated after 48 hof hypoxiatreatment (Figure S4B and S4C). Importantly, 48 h of hypoxia resulted in a marked accumulation of TFEB proteinin the cytoplasmic subfraction, with a corresponding decline in thenuclear subfraction (Figure S4D).Furthermore, immunostaining detectionrevealed that the majority of TFEB protein existed in the nucleus after 6 h of hypoxia treatment, whereas it was mainly in the cytosol after 48 h of hypoxia treatment (Figure S4A). Then,we used GV492 particles that encodetheUbi promoter-drivenconstruct to transduce TFEB into the GC-2 cells under hypoxia exposure. Immunofluorescence, immunoblot and RT-qPCRanalysis confirmedthat the endogenousTFEB expression in the GC-2 cells was specifically up-regulated comparedwith thoseGFP-tagged Lenti-NC vector, especiallyin the hypoxia-treated group(Figure 3A, 3B and 3C). Overexpression of TFEB significantly reversed the decrease in the transcriptional and protein levels of V-ATPase after 48 h of hypoxia exposure (Figure 3Band3C). Thesedata indicated that prolonghypoxia caused the deactivation of TFEB, especially in GC-2 cells, as indicated by the decreasedexpression and translocation to nuclei.TFEB overexpression resulted in an evident increase in the expression of V-ATPase.

4. V-ATPase deficiency induced the apoptosis of GC-2 cells via DR5 signaling

We have previously found that hypoxia can enhancethe apoptosis of GC-2 cells by inhibitingV-ATPase [20]. However, whether V-ATPase was involved in regulating DR_5 (Death Receptor 5, a key molecule of extrinsic apoptosis pathway) remained unclear. To this end, we knocked down the expression of endogenous V-ATPaseby using siRNAin order to detect the expression of extrinsic apoptosis-related markers in GC-2 cells. The results of FCM analysis showed that hypoxia alone induced 15.75%of apoptosis, whereashypoxia combinedwithsiV-ATPase augmented apoptosis to 27.15%(Fig. 4A).

Furthermore, there was a significant increase in the mRNA level of DR_5 in GC-2 cellsafter being treated with 1% oxygen for 48 h(Fig. 4B). Similarly, V-ATPase deficiency induced an increase in the levels of DR_5 and caspase-8 (Key effector of extrinsic apoptosis pathway) (Fig. 4C).These data indicated that V-ATPase deficiency enhances the extrinsic apoptosis pathway in GC-2 cells exposed to hypoxia.

5. Overexpression of V-ATPase ameliorated the apoptosis of GC-2 cells via DR5 signaling

We next sought to investigate the important roles of V-ATPaseaffecting the apoptosis of GC-2 cells.We overexpressed V-ATPase by lentivirus transfection and detected the apoptosis of GC-2 cells by TUNEL and FCM assay. The results showed decreased TUNEL-positive puncta in GC-2 cells were pretreated by V-ATPase overexpression (Fig. 5A). The FCM assay results wereconsistent with the results of the TUNEL staining (Fig. 5B). Meanwhile, overexpression of V-ATPase resulted in an evident reduction in the expressions of DR_5 and caspase-8 (Fig. 5C). Collectively, these results suggested that V-ATPase might be a critical negative regulator of spermatogenesis by influencingtheextrinsic apoptosis pathway of spermatocytes.

6. Hypoxia-induced V-ATPase deficiency promoted GC-2 apoptosis via activation of JNK/c-Jun pathway

To further elucidate the underlying mechanism of V-ATPase deficiency facilitating the apoptosis of GC-2 cells, we performed RNA-seq on GC-2 cells by inducing V-ATPase deficiency through hypoxia exposure.Total 1084 and 1350 genes were consistently up-regulated or down-regulated in GC-2 cells with hypoxia exposure, respectively(Figure S5A). Kyoto Encyclopedia of Genes and Genomes (KEGG) analysis suggested hypoxia triggered MAPK (mitogen-activated protein kinase) signaling pathway (Figure S5B). A set of genes that codepositive mediators of JNK (A key member of the MAPK family) signaling pathway including MAPK8 (c-Jun N-terminal kinase 1, or JNK1), Jun (orc-Jun), HSF1, Rho, SHC4, CrkL, SOS1, Smad4, Atf2, bax and TRAF2were up-regulated consecutively (Figure S5B). Further RT-qPCR and western blotvalidated thatphosphorylation of JNK and c-Jun expression wereincreased in GC-2 cells under hypoxia(Fig. 6A and 6B). Taken together, these findings indicated that hypoxia induced the activation of JNK signaling.

Several studies have reported that the JNK signalling pathway is associated with the expression of DR (Death Receptor) markers and apoptosis [35, 36]. To reveal the underlying mechanisms by which V-ATPase deficiency promotes apoptosis, we knocked down or overexpressed V-ATPase in GC-2 cells and analysed the protein expression of total and phosphorylated JNK and c-Jun by western blot. In V-ATPase overexpressed GC-2 cells, the expression of phosphorylated JNK and c-Jun were significantly decreased compared to CTL siRNA cells. However, knockdown of V-ATPase in GC-2 cells increased the phosphorylation of JNK and c-Jun (Figure 6C). Furthermore, to explore the role of JNK activation in V-

ATPase deficiency-induced apoptosis, we examined the effect of V-ATPase deficiency on the expression of DR related markers in the presence or absence of c-Jun siRNA. The decreased expression of death receptor (DR) related marker of DR5 and caspase-8 exhibited that c-Jun siRNA relieved expression of DR related marker after V-ATPase deficiency (Fig. 6D). The data indicated that the JNK signalling pathway mediated V-ATPase-regulated apoptosis in GC-2 cells.

7. JNK/c-Jun pathway deficiency attenuated spermatogenesis reduction induced by V-ATPase deficiency in mice under hypoxia condition

Above findings indicated that V-ATPase inhibits apoptosis activation in vitro via inhibiting the JNK/c-Jun pathway. Next, to examine whether depletion of c-Jun rescued spermatogenesis in vivo, we knocked down the expression of endogenous c-Jun using siRNA to investigate the damage of seminiferous tubules in mice by H&E, TUNEL and western blot assays. We found that mice transfected with the CTL siRNA demonstrated degeneration and detachment of spermatocytes. In contrast, c-Jun siRNA-transfected mice showed a considerable reduction in apoptosis of spermatocytes(Figure S6A and S6B). Consistent with the results of TUNEL assay, analysis of sperm count showed that the number of mice receiving c-Jun siRNA was significantly higher than that of CTL siRNA.(Figure 7A). Meanwhile, the testis in CTL siRNA mice showed high expression of DR_5 and caspase-8, whilec-Jun depletion barely expressed DR_5 and caspase-8 in testis. Moreover, c-Jun depletion inhibited the expression of DR-related marker DR5 and caspase-8 (Fig. 7B). These data indicated that c-Jun depletion rescues spermatogenesis in testis and inhibits the expression of DR-related markers after hypoxia exposure.

Discussion

It has been reported that hypoxia induced spermatogenesis reduction caused by spermatocyte apoptosis in mice [4, 5, 37]. Continuous autophagic flux play a prosurvival role in spermatocyte cells by directly inhibiting apoptosis of spermatocytes [38]. Previously, we demonstrated that serious hypoxia inhibited autophagic flux by downregulating the expression of V-ATPase in GC-2 cells [20]. In the present study, we determined that V-ATPase deficiency resulted in more severe spermatogenesis deficits after hypoxia exposure in mice. These deficits were associated with exacerbation of spermatocyte apoptosis. These results indicated V-ATPase may exert a protective role against spermatogenesis reduction via the suppression of the apoptosis of spermatocyte. However, the mechanism by which V-ATPase inhibiting apoptosis of spermatocytes is still poorly understood.

So far, studies indicate that the main causeof spermatocyte apoptosis induced by V-ATPase deficiency is the generation of immature autophagosome resultsfrom the decreaseof autophagic flux under hypoxia stimulation, which in turn promotes the caspase-8 and death receptor (DR-) apoptosis pathway [20]. Here,wefoundthat the DR-apoptotic marker DR5 and effector caspase-8 accumulated with prolong

hypoxia, which was consistent with gradual reduction of autolysosome marker V-ATPase. We have observed the decrease of lysosomal synthesis in GC-2 cells under hypoxia exposure, including the decrease of the expression of lysosomal marker LAMP2 and the decrease of the ratio of lysosomes to cells. Whether the decreased V-ATPase expression after hypoxia is connected with the observed lysosome biogenesisdefects remains to be determined.

Since TFEB was recently discovered as a major regulator oflysosome biogenesis as well as being a potential therapeutic target torescue myocardial ischemic injury and neurodegeneration[39, 40], we are interested in its role in regulating V-ATPase and spermatocyte apoptosis. Inthepresentstudy,itisnotedthatat 48 hafter hypoxia exposure boththemRNAandtotalproteinlevelofTFEBweresignificantly down-regulated.Additionally,therewasmarked reduction ofTFEBproteininthenuclearsubfraction,suggestingthattherewas reduced translocationofTFEBintothenucleusfrom 24hto 48hafter hypoxia. On the contrary, we conducted LV-mediated GC2-specific overexpression of TFEB to show thatoverexpression of TFEB was effective in reversing the hypoxia-induced reduction of autolysosome marker V-ATPase.The results obtained in this study supporttheprevious suggestion that TFEB might regulate lysosomal biosynthesis.

The V-ATPase was ATP-dependent proton pumps that acidify intracellular compartments and ubiquitously expressed in mammals. The V-ATPase was extensively studied in cancer and neurodegenerative disease. Recent work has supported the concept that the V-ATPase playspro-survival role in cancers [41–43]. A number of studies have shown theoverexpression of V-ATPase subunits in various cancer cell lines and tumor samples, including breast, prostate, pancreatic, colorectal, liver, lung, ovarian, stomach, esophageal cancers and melanoma, where it showed thepro-tumoral activity[44–52]. In contrast, induction of apoptosis by V-ATPase inhibition has beenreported in both human and murine models encompassingmany tumor types.Tumor cells are more sensitive to V-ATPase-inhibition-dependent cancer cell death, and loss of V-ATPase activity reduces cancer cell growth [53]. Additionally, archazolid can induce p53 (tumor suppressor) protein levels by inhibitingV-ATPase expressionin cancer cells [54]. It has also been shown that V-ATPase inhibition differentially affects regulation of AMPK in tumor and nontumor cells, and that this differential regulation contributes to the selectivity of V-ATPase inhibitors for tumor cells[55]. Cancer-associated V-ATPase significantly induced the life span of protumor genic neutrophils by activating the intrinsic pathway of apoptosis[56]. ECDD-S27 retards the autophagy pathway by inhibiting the V-ATPase and restricts cancer cell survival[57]. Some study has found that intracellular acidosis caused by V-ATPase inhibition in breast cancer cells stabilizes the expression of the pro-apoptotic protein Bnip3, resulting in cell death [58]. It has also recently been demonstrated that treatment of breast cancer cells with the V-ATPase inhibitor archazolid disrupts the internalization of the transferrin receptor, leading to iron deprivation and subsequent apoptosis [59]. In our study, using V-ATPase lentivirus for the first time as tool, we found thatV-ATPase overexpression caused the decline of apoptosis in GC-2 cells. Of interest, in contrast to GC-2 cells that deplete V-ATPase, V-ATPase overexpression induces the survival of V-ATPase overexpressed GC-2 cells. Similarly, in vitro studies revealed that V-ATPase reduces the apoptosis of non-cancer cells, including rat proximal tubular cells, neuronal cell and osteoclast[60–62]. Genetic analysis of individuals with X-linked Parkinson Disease with

Spasticity (XPDS) yielded a novel candidate gene locus on the X chromosome, and it was later shown that a point mutation (c.345C > T) in exon 4 of the ATP6AP2 gene causes altered splicing of ATP6AP2 in XPDS[63]. It has been reported that in Cln1-/- mice, palmitoyl-protein thioesterase-1 (PPT1)adversely affectedV-ATPase function and dysregulated lysosomal acidification in other lysosomal storage disorders (LSDs) and common neurodegenerative diseases[64].Of note, we used GC-2 cells with V-ATPase silencing or overexpressed under hypoxia treatment to show for the first time that V-ATPase in GC-2 cells regulates apoptosis of spermatocyte by acting on DR-apoptosis pathway.

It has been found that V-ATPase wasclosely associated with multiple signal transduction signaling, such as m-TOR (mammalian Target OfRapamycin), Wnt, TGF-β, Notch,G protein-coupled receptors (GPCRs) and receptortyrosine kinases (RTKs), etc. Several critical pathways of growth,survival and differentiation that are frequently altered incancers rely on the V-ATPase[65]. In Notch signaling, the Notch receptoriscleaved in Golgi and translocated to the plasma membrane, where further cleavage of the receptor occurs in response to Notch ligand binding. Cleaved Notch intracellular domain is translocated to nucleus and activates Notch target genes[66]. TGF-βprotein is glycosylated in theGolgi to form mature TGF-βand secreted into the extracellular space.TGF-βbinds to its receptor (TGF-βR)andleads to the endocytosis andphosphorylation of Smad2, which in turn activates TGF-βtarget genes[67]. During canonical Wnt signaling, the binding of ligands to the Wntreceptor complex inhibits the phosphorylation of β-catenin by GSK-3β and directs the translocation ofβ-catenin into thenucleus, where it activates the transcription of target genes Cyclin D1 and oncogene c-Myc[68]. In addition, it was found that V-ATPase is critical for sensing of amino acids and subsequent activation of mTOR complex 1 (mTORC1). Amino acids stimulate recruitment of mTORC1 to the lysosomal surface, where its direct activator,Ragulator(a family of four GTPases that are related to Ras, RagGTPases) was associatedtightly with the V-ATPase[69, 70].

V-ATPase-mediated acidification can affect signaling in thefollowing ways: (a) Maturation of signaling molecules Notch receptor and TGF-βbyfurin glycosylationin the golgi vesicles. (b) Cleavage and activationof pathway mediators by acid-dependent enzyme like matrix metallo proteinases (MMPs) and γ-secretase. (c) Maintenance of basal signaling byrecycling endocytosis of both ligand and receptor. (d)Degradation of signaling molecules in lysosomes. In our research, by RNA-seq analysis of transcription factors that arepotentially involved in induction of DR5 expression. We found thatV-ATPase overexpression induced down-regulation of phosphorylation/activation of JNK (c-Jun N-terminal kinase, MAPK8) signaling molecules.Instead, phosphorylation of JNK1 andthe nuclear translocation of c-Jun were markedly promotedby V-ATPase deficiency, which was consistent withtheactivation of JNK signaling in glial cells, monocyte-derived macrophages and RAW 264[71–73]. Moreover, some other studies have shown that V-ATPase inhibits JNK pathway in drosophila epithelium, mouse bone marrow macrophages and osteoclast [74–76]. The exact mechanism by which V-ATPase acts on glycosylation, MMPs, γ-secretase, endocytosis and degradation in V-ATPase-mediated JNK signaling still needs further investigation.

The JNK, as a MAPK member, regulates various cell functions, such as proliferation, apoptosis, and differentiation[77]. The mechanism underlying JNK-regulated DR-apoptotic pathway has been largely investigated in cancer cells. It has been demonstrated that erinacine A induces apoptosis by acting JNK, p300, and NFκBp50signaling molecules and an increasingthe cellular transcriptional levels of TNFR, Fas, and FasL[78]. The attenuation of ERK1/2 phosphorylation accompanied by the activation of JNK was detected in D. bulbifera ethyl acetate fraction (DBEAF)-induced activation of death receptor, Fas and HCT116 cell apoptosis [79]. The capsular polysaccharide induced extrinsic cell apoptosis by up-regulating FAS/FASL signaling proteins and cleaved-caspase-8 and promoted a ROS-dependent intrinsic cell apoptosis by activating a JNK and p38 signaling but not ERK1/2 signaling of mitogen-activated protein kinases (MAPK) pathways[80]. The JNK inhibition was validated to block irradiation-induced FasL expression, which was critical in determining non-irradiated hepatocyte injury[81].Short hairpin RNA (shRNA)-mediated knockdown of JNK confirmed its key role in the regulation of sensitivity to this combination as cells with suppressed JNK expression exhibited significantly reduced TRAIL/sunitinib-mediatedcolon cancer apoptosis[82]. Subcutaneous tumor growth analysis revealed that Mucosa-associated lymphoma antigen 1 (a lymphoma oncogene, MALT1) gene silencing significantly increased melanoma apoptosis and forced expression of the c-Jun upstream activator MKK7[83]. Quercetin activated c-Jun N-terminal kinase (JNK) in a dose-dependent manner, which in turn induced the proteasomal degradation of cFLIP, and JNK activation also sensitized pancreatic cancer cells to TRAIL-induced apoptosis[84].Tanshinone IIA (antitumor drug, TIIA) promoted JNK-mediated signaling to up-regulated CHOP and thereby inducing DR5 expression as shown by the ability of a JNK inhibitor to potently suppress the TIIA-mediated activation of CHOP and DR5[36].Saikosaponin D (antitumor drug) alone or in combination with SP600125 (JNK inhibitor) activated caspase-3, -8 in human osteosarcoma U2 cells[85]. Inthe present study,the activation of JNK/c-Jun in spermatocyte was enhanced by V-ATPase deficiency in vitro, while inhibitionof JNK phosphorylation alleviated spermatocyte apoptosis, therebyindicating that V-ATPase attenuates spermatocyte apoptosis,at least in part, via the suppression of the JNK/c-Jun pathwayafter hypoxia exposure.

Emerging studies demonstrated thatJNK signaling regulates non-cancer cell apoptosis induced by ischemic hypoxia, including neuronal, astrocyte and cardiomyocyte [86–88]. Various JNK-related synthetic inhibitors have been reported in ischemic hypoxia injury, such as micromolecules SP600125 and IQ-1S. It has been reported that SP600125 treatment inhibits JNK activation and provides neuroprotection in ischemia/reperfusion via inhibiting neuronal apoptosis[89]. IQ-1S releases nitric oxide in the course of redox biological transformation process and improves the results of stroke in a cerebral reperfusion mouse model[90]. In this study, our data provides evidence that V-ATPase deficiency leads to increased phosphorylation of JNK/c-Jun in GC-2 cells under hypoxia exposure. In addition, the V-ATPase deficiency-induced phosphorylation of JNK/c-Jun and the cell apoptosis activity was reduced when c-Jun was inhibited by RNA interference (RNAi). Our data suggest that JNK activation might be a key event in V-ATPase-mediated apoptosis in GC-2 cells.

In conclusion, V-ATPase deficiency aggravates spermatogenesis deficits under hypoxia exposure, which may be due to the exacerbation ofspermatocyte apoptosis. The aggravated spermatocyte damage is

associated withenhanced DR-apoptotic pathway activation, which is mediated by V-ATPase via the JNK/c-Jun signal. These results demonstrate the protective role of the V-ATPase against spermatocyteinjury andprovide evidence for the exploration of V-ATPase-based treatmentsfor hypoxia-induced spermatogenesis reduction**(Figure 8)**.

Abbreviations

V-ATPase, Vacuolar H^+-ATPase; JNK, c-Jun N-terminal kinase; DR_5,Death Receptor 5; FCM, Method of flow cytometry; TNF, Tumour necrosis factor; mTOR, mammalian Target Of Rapamycin; SAPK,Stress-activatedprotein kinase; MAPK, Mitogen-activated protein kinase; PPT1, palmitoyl-protein thioesterase-1; LSDs, Lysosomal storage disorders; GPCRs, G protein-coupled receptors; RTKs, Receptortyrosine kinases; MMPs, Matrix metallo proteinases; DBEAF, D. bulbifera ethyl acetate fraction; MALT1, Mucosa-associated lymphoma antigen 1; MKK, MAP Kinase Kinase; RNAi, RNA interference; TRAIL, Tumor necrosis factor-related apoptosis-inducing ligand; TUNEL, Terminal deoxynucleotidyl transferase mediated dUTP nick end-labeling; c-FLIP, cellular Fas-associated death domain-like interleulin-1βconverting enzyme inhibitory protein; BNIP-3, $Bcl-_2$ nineteen-kilodalton interacting protein 3; $Bcl-_2$, B-cell lymphoma gene-2

Declarations

Ethics approval and consent to participate

Approval was obtained from the laboratory animal welfare and ethics committee of the third military medical university. The procedures used in this study adhere to the tenets of the Declaration of Helsinki. Informed consent was obtained from all individual participants included in the study.

Consent for publication:

The participant has consented to the submission of the case report to the journal. The authors declare that they have no conflict of interest.

Availability of data and material: h

ttps://www.ncbi.nlm.nih.gov/bioproject/?term=PRJNA608077

Funding:

This work was supported by the National Natural Science Foundation of China (81701855)

Authors' contributions:

Fei Han, Email: han16897723@163.com

Acknowledgements:

None

References

1. Krausz, C. and A. Riera-Escamilla, *Genetics of male infertility.* Nat Rev Urol, 2018. **15**(6): p. 369-384.
2. Liu, K., et al., *Role of genetic mutations in folate-related enzyme genes on Male Infertility.* Sci Rep, 2015. **5**: p. 15548.
3. Meng, X., et al., *Genetic Deficiency of Mtdh Gene in Mice Causes Male Infertility via Impaired Spermatogenesis and Alterations in the Expression of Small Non-coding RNAs.* J Biol Chem, 2015. **290**(19): p. 11853-64.
4. Liao, W., et al., *Hypobaric hypoxia causes deleterious effects on spermatogenesis in rats.* Reproduction, 2010. **139**(6): p. 1031-8.
5. Yin, J., et al., *Hypoxia-induced apoptosis of mouse spermatocytes is mediated by HIF-1alpha through a death receptor pathway and a mitochondrial pathway.* J Cell Physiol, 2017.
6. Chao, X., et al., *Impaired TFEB-Mediated Lysosome Biogenesis and Autophagy Promote Chronic Ethanol-Induced Liver Injury and Steatosis in Mice.* Gastroenterology, 2018. **155**(3): p. 865-879 e12.
7. Wang, Y., et al., *Acetyltransferase GCN5 regulates autophagy and lysosome biogenesis by targeting TFEB.* EMBO Rep, 2020. **21**(1): p. e48335.
8. Shao, Q., et al., *C9orf72 and smcr8 mutant mice reveal MTORC1 activation due to impaired lysosomal degradation and exocytosis.* Autophagy, 2019: p. 1-16.
9. Mindell, J.A., *Lysosomal acidification mechanisms.* Annu Rev Physiol, 2012. **74**: p. 69-86.
10. Kinouchi, K., et al., *The (pro)renin receptor/ATP6AP2 is essential for vacuolar H+-ATPase assembly in murine cardiomyocytes.* Circ Res, 2010. **107**(1): p. 30-4.
11. Kinouchi, K., et al., *The role of individual domains and the significance of shedding of ATP6AP2/(pro)renin receptor in vacuolar H(+)-ATPase biogenesis.* PLoS One, 2013. **8**(11): p. e78603.
12. Kissing, S., et al., *Disruption of the vacuolar-type H(+)-ATPase complex in liver causes MTORC1-independent accumulation of autophagic vacuoles and lysosomes.* Autophagy, 2017. **13**(4): p. 670-685.
13. Dechant, R., et al., *Cytosolic pH regulates cell growth through distinct GTPases, Arf1 and Gtr1, to promote Ras/PKA and TORC1 activity.* Mol Cell, 2014. **55**(3): p. 409-21.
14. Bar-Peled, L., et al., *Ragulator is a GEF for the rag GTPases that signal amino acid levels to mTORC1.* Cell, 2012. **150**(6): p. 1196-208.

15. Jewell, J.L., et al., *Metabolism. Differential regulation of mTORC1 by leucine and glutamine.* Science, 2015. **347**(6218): p. 194-8.
16. Yang, Y. and D.J. Klionsky, *A novel role of UBQLNs (ubiquilins) in regulating autophagy, MTOR signaling and v-ATPase function.* Autophagy, 2020. **16**(1): p. 1-2.
17. Zoncu, R., et al., *mTORC1 senses lysosomal amino acids through an inside-out mechanism that requires the vacuolar H(+)-ATPase.* Science, 2011. **334**(6056): p. 678-83.
18. Hou, W., et al., *Autophagic degradation of active caspase-8: a crosstalk mechanism between autophagy and apoptosis.* Autophagy, 2010. **6**(7): p. 891-900.
19. Amir, M., et al., *Inhibition of hepatocyte autophagy increases tumor necrosis factor-dependent liver injury by promoting caspase-8 activation.* Cell Death Differ, 2013. **20**(7): p. 878-87.
20. Yin, J., et al., *Elevation of autophagy rescues spermatogenesis by inhibiting apoptosis of mouse spermatocytes.* Reproduction, 2018.
21. Liu, X., et al., *Correction to: Celastrol mediates autophagy and apoptosis via the ROS/JNK and Akt/mTOR signaling pathways in glioma cells.* J Exp Clin Cancer Res, 2019. **38**(1): p. 284.
22. Liu, X., et al., *Celastrol mediates autophagy and apoptosis via the ROS/JNK and Akt/mTOR signaling pathways in glioma cells.* J Exp Clin Cancer Res, 2019. **38**(1): p. 184.
23. Hu, L., et al., *Hsp90 Inhibitor SNX-2112 Enhances TRAIL-Induced Apoptosis of Human Cervical Cancer Cells via the ROS-Mediated JNK-p53-Autophagy-DR5 Pathway.* Oxid Med Cell Longev, 2019. **2019**: p. 9675450.
24. Bai, Y., et al., *PDIA6 modulates apoptosis and autophagy of non-small cell lung cancer cells via the MAP4K1/JNK signaling pathway.* EBioMedicine, 2019. **42**: p. 311-325.
25. Wang, Z., et al., *Schisantherin A induces cell apoptosis through ROS/JNK signaling pathway in human gastric cancer cells.* Biochem Pharmacol, 2019: p. 113673.
26. Zhao, Q., et al., *Pristimerin induces apoptosis and autophagy via activation of ROS/ASK1/JNK pathway in human breast cancer in vitro and in vivo.* Cell Death Discov, 2019. **5**: p. 125.
27. Tan, B., et al., *Bruceine D induces apoptosis in human non-small cell lung cancer cells through regulating JNK pathway.* Biomed Pharmacother, 2019. **117**: p. 109089.
28. Kopalli, S.R., et al., *Pectinase-treated Panax ginseng ameliorates hydrogen peroxide-induced oxidative stress in GC-2 sperm cells and modulates testicular gene expression in aged rats.* J Ginseng Res, 2016. **40**(2): p. 185-95.
29. Naldini, L., et al., *In vivo gene delivery and stable transduction of nondividing cells by a lentiviral vector.* Science, 1996. **272**(5259): p. 263-7.
30. Tiscornia, G., O. Singer, and I.M. Verma, *Production and purification of lentiviral vectors.* Nat Protoc, 2006. **1**(1): p. 241-5.
31. Shetty, S.D. and L.K. Bairy, *Effect of sorafenib on sperm count and sperm motility in male Swiss albino mice.* J Adv Pharm Technol Res, 2015. **6**(4): p. 165-9.

32. Picelli, S., et al., *Full-length RNA-seq from single cells using Smart-seq2.* Nat Protoc, 2014. **9**(1): p. 171-81.
33. Altermann, E. and T.R. Klaenhammer, *PathwayVoyager: pathway mapping using the Kyoto Encyclopedia of Genes and Genomes (KEGG) database.* BMC Genomics, 2005. **6**: p. 60.
34. Tognon, E., et al., *Control of lysosomal biogenesis and Notch-dependent tissue patterning by components of the TFEB-V-ATPase axis in Drosophila melanogaster.* Autophagy, 2016. **12**(3): p. 499-514.
35. Nazim, U.M. and S.Y. Park, *Luteolin sensitizes human liver cancer cells to TRAILinduced apoptosis via autophagy and JNKmediated death receptor 5 upregulation.* Int J Oncol, 2019. **54**(2): p. 665-672.
36. Chang, C.C., et al., *Tanshinone IIA Facilitates TRAIL Sensitization by Up-regulating DR5 through the ROS-JNK-CHOP Signaling Axis in Human Ovarian Carcinoma Cell Lines.* Chem Res Toxicol, 2015. **28**(8): p. 1574-83.
37. Reyes, J.G., et al., *The hypoxic testicle: physiology and pathophysiology.* Oxid Med Cell Longev, 2012. **2012**: p. 929285.
38. Yin, J., et al., *Regulatory effects of autophagy on spermatogenesis.* Biol Reprod, 2017. **96**(3): p. 525-530.
39. Sciarretta, S., et al., *Trehalose-Induced Activation of Autophagy Improves Cardiac Remodeling After Myocardial Infarction.* J Am Coll Cardiol, 2018. **71**(18): p. 1999-2010.
40. Liu, Y., et al., *Neuronal-targeted TFEB rescues dysfunction of the autophagy-lysosomal pathway and alleviates ischemic injury in permanent cerebral ischemia.* Autophagy, 2019. **15**(3): p. 493-509.
41. Cotter, K., et al., *Recent Insights into the Structure, Regulation, and Function of the V-ATPases.* Trends Biochem Sci, 2015. **40**(10): p. 611-622.
42. Kitazawa, S., et al., *Cancer with low cathepsin D levels is susceptible to vacuolar (H(+))-ATPase inhibition.* Cancer Sci, 2017. **108**(6): p. 1185-1193.
43. Kuchuk, O., et al., *pH regulators to target the tumor immune microenvironment in human hepatocellular carcinoma.* Oncoimmunology, 2018. **7**(7): p. e1445452.
44. Couto-Vieira, J., et al., *Multi-cancer V-ATPase molecular signatures: A distinctive balance of subunit C isoforms in esophageal carcinoma.* EBioMedicine, 2020. **51**: p. 102581.
45. Kim, B.K., et al., *Bcl-2-dependent synthetic lethal interaction of the IDF-11774 with the V0 subunit C of vacuolar ATPase (ATP6V0C) in colorectal cancer.* Br J Cancer, 2018. **119**(11): p. 1347-1357.
46. Collins, M.P. and M. Forgac, *Regulation of V-ATPase Assembly in Nutrient Sensing and Function of V-ATPases in Breast Cancer Metastasis.* Front Physiol, 2018. **9**: p. 902.
47. Nardi, F., et al., *Lipid droplet velocity is a microenvironmental sensor of aggressive tumors regulated by V-ATPase and PEDF.* Lab Invest, 2019. **99**(12): p. 1822-1834.
48. Gu, D., et al., *The asialoglycoprotein receptor suppresses the metastasis of hepatocellular carcinoma via LASS2-mediated inhibition of V-ATPase activity.* Cancer Lett, 2016. **379**(1): p. 107-16.

49. Kim, Y.S., et al., *Silencing of secretory clusterin sensitizes NSCLC cells to V-ATPase inhibitors by downregulating survivin.* Biochem Biophys Res Commun, 2018. **495**(2): p. 2004-2009.
50. Kulshrestha, A., et al., *Selective inhibition of tumor cell associated Vacuolar-ATPase 'a2' isoform overcomes cisplatin resistance in ovarian cancer cells.* Mol Oncol, 2016. **10**(6): p. 789-805.
51. Liu, P., et al., *Expression and role of V1A subunit of V-ATPases in gastric cancer cells.* Int J Clin Oncol, 2015. **20**(4): p. 725-35.
52. Martins, B.X., et al., *Myrtenal-induced V-ATPase inhibition - A toxicity mechanism behind tumor cell death and suppressed migration and invasion in melanoma.* Biochim Biophys Acta Gen Subj, 2019. **1863**(1): p. 1-12.
53. McGuire, C., et al., *Regulation of V-ATPase assembly and function of V-ATPases in tumor cell invasiveness.* Biochim Biophys Acta, 2016. **1857**(8): p. 1213-1218.
54. Schneider, L.S., et al., *MDM2 antagonist nutlin-3a sensitizes tumors to V-ATPase inhibition.* Mol Oncol, 2016. **10**(7): p. 1054-62.
55. Bartel, K., R. Muller, and K. von Schwarzenberg, *Differential regulation of AMP-activated protein kinase in healthy and cancer cells explains why V-ATPase inhibition selectively kills cancer cells.* J Biol Chem, 2019. **294**(46): p. 17239-17248.
56. Ibrahim, S.A., et al., *Cancer-associated V-ATPase induces delayed apoptosis of protumorigenic neutrophils.* Mol Oncol, 2020.
57. Paha, J., et al., *A novel potent autophagy inhibitor ECDD-S27 targets vacuolar ATPase and inhibits cancer cell survival.* Sci Rep, 2019. **9**(1): p. 9177.
58. Graham, R.M., J.W. Thompson, and K.A. Webster, *Inhibition of the vacuolar ATPase induces Bnip3-dependent death of cancer cells and a reduction in tumor burden and metastasis.* Oncotarget, 2014. **5**(5): p. 1162-73.
59. Schneider, L.S., et al., *Vacuolar-ATPase Inhibition Blocks Iron Metabolism to Mediate Therapeutic Effects in Breast Cancer.* Cancer Res, 2015. **75**(14): p. 2863-74.
60. Hirose, T., et al., *ATP6AP2 variant impairs CNS development and neuronal survival to cause fulminant neurodegeneration.* J Clin Invest, 2019. **129**(5): p. 2145-2162.
61. Song, X.B., et al., *Autophagy blockade and lysosomal membrane permeabilization contribute to lead-induced nephrotoxicity in primary rat proximal tubular cells.* Cell Death Dis, 2017. **8**(6): p. e2863.
62. Yao, J., et al., *Protein kinase C inhibitor, GF109203X attenuates osteoclastogenesis, bone resorption and RANKL-induced NF-kappaB and NFAT activity.* J Cell Physiol, 2015. **230**(6): p. 1235-42.
63. Korvatska, O., et al., *Altered splicing of ATP6AP2 causes X-linked parkinsonism with spasticity (XPDS).* Hum Mol Genet, 2013. **22**(16): p. 3259-68.
64. Bagh, M.B., et al., *Misrouting of v-ATPase subunit V0a1 dysregulates lysosomal acidification in a neurodegenerative lysosomal storage disease model.* Nat Commun, 2017. **8**: p. 14612.
65. Pamarthy, S., et al., *The curious case of vacuolar ATPase: regulation of signaling pathways.* Mol Cancer, 2018. **17**(1): p. 41.

66. Wissel, S., et al., *Time-resolved transcriptomics in neural stem cells identifies a v-ATPase/Notch regulatory loop.* J Cell Biol, 2018. **217**(9): p. 3285-3300.
67. Pamarthy, S., et al., *The V-ATPase a2 isoform controls mammary gland development through Notch and TGF-beta signaling.* Cell Death Dis, 2016. **7**(11): p. e2443.
68. Jung, Y.S., et al., *TMEM9 promotes intestinal tumorigenesis through vacuolar-ATPase-activated Wnt/beta-catenin signalling.* Nat Cell Biol, 2018. **20**(12): p. 1421-1433.
69. Wang, F., et al., *Follicular lymphoma-associated mutations in vacuolar ATPase ATP6V1B2 activate autophagic flux and mTOR.* J Clin Invest, 2019. **130**: p. 1626-1640.
70. Abu-Remaileh, M., et al., *Lysosomal metabolomics reveals V-ATPase- and mTOR-dependent regulation of amino acid efflux from lysosomes.* Science, 2017. **358**(6364): p. 807-813.
71. Thomas, L., et al., *Selective upregulation of TNFalpha expression in classically-activated human monocyte-derived macrophages (M1) through pharmacological interference with V-ATPase.* Biochem Pharmacol, 2017. **130**: p. 71-82.
72. Byun, Y.J., et al., *Vacuolar H+ -ATPase c protects glial cell death induced by sodium nitroprusside under glutathione-depleted condition.* J Cell Biochem, 2011. **112**(8): p. 1985-96.
73. Kamachi, F., et al., *Involvement of Na+/H+ exchangers in induction of cyclooxygenase-2 by vacuolar-type (H+)-ATPase inhibitors in RAW 264 cells.* FEBS Lett, 2007. **581**(24): p. 4633-8.
74. Petzoldt, A.G., et al., *Elevated expression of the V-ATPase C subunit triggers JNK-dependent cell invasion and overgrowth in a Drosophila epithelium.* Dis Model Mech, 2013. **6**(3): p. 689-700.
75. Jiao, Z., et al., *Kaempferide Prevents Titanium Particle Induced Osteolysis by Suppressing JNK Activation during Osteoclast Formation.* Sci Rep, 2017. **7**(1): p. 16665.
76. Yin, Z., et al., *Glycyrrhizic acid suppresses osteoclast differentiation and postmenopausal osteoporosis by modulating the NF-kappaB, ERK, and JNK signaling pathways.* Eur J Pharmacol, 2019. **859**: p. 172550.
77. Chen, X., et al., *Activation of AMPK inhibits inflammatory response during hypoxia and reoxygenation through modulating JNK-mediated NF-kappaB pathway.* Metabolism, 2018. **83**: p. 256-270.
78. Lee, K.C., et al., *Induction Apoptosis of Erinacine A in Human Colorectal Cancer Cells Involving the Expression of TNFR, Fas, and Fas Ligand via the JNK/p300/p50 Signaling Pathway With Histone Acetylation.* Front Pharmacol, 2019. **10**: p. 1174.
79. Ahmad Hidayat, A.F., et al., *Dioscorea bulbifera induced apoptosis through inhibition of ERK 1/2 and activation of JNK signaling pathways in HCT116 human colorectal carcinoma cells.* Biomed Pharmacother, 2018. **104**: p. 806-816.
80. Jiang, Z., et al., *Capsular Polysaccharide of Mycoplasma ovipneumoniae Induces Sheep Airway Epithelial Cell Apoptosis via ROS-Dependent JNK/P38 MAPK Pathways.* Oxid Med Cell Longev, 2017. **2017**: p. 6175841.
81. Dong, Y., et al., *Activation of the JNK-c-Jun pathway in response to irradiation facilitates Fas ligand secretion in hepatoma cells and increases hepatocyte injury.* J Exp Clin Cancer Res, 2016. **35**(1): p.

114.

82. Mahalingam, D., et al., *Heightened JNK Activation and Reduced XIAP Levels Promote TRAIL and Sunitinib-Mediated Apoptosis in Colon Cancer Models.* Cancers (Basel), 2019. **11**(7).
83. Wang, Y., et al., *MALT1 promotes melanoma progression through JNK/c-Jun signaling.* Oncogenesis, 2017. **6**(7): p. e365.
84. Kim, J.H., et al., *Quercetin sensitizes pancreatic cancer cells to TRAIL-induced apoptosis through JNK-mediated cFLIP turnover.* Int J Biochem Cell Biol, 2016. **78**: p. 327-334.
85. Gao, T., et al., *Use of Saikosaponin D and JNK inhibitor SP600125, alone or in combination, inhibits malignant properties of human osteosarcoma U2 cells.* Am J Transl Res, 2019. **11**(4): p. 2070-2080.
86. Zheng, J., et al., *JNK-IN-8, a c-Jun N-terminal kinase inhibitor, improves functional recovery through suppressing neuroinflammation in ischemic stroke.* J Cell Physiol, 2020. **235**(3): p. 2792-2799.
87. Huang, W., et al., *Paracrine Factors Secreted by MSCs Promote Astrocyte Survival Associated With GFAP Downregulation After Ischemic Stroke via p38 MAPK and JNK.* J Cell Physiol, 2015. **230**(10): p. 2461-75.
88. Xu, J., et al., *Mitochondrial JNK activation triggers autophagy and apoptosis and aggravates myocardial injury following ischemia/reperfusion.* Biochim Biophys Acta, 2015. **1852**(2): p. 262-70.
89. Shao, S., et al., *Atorvastatin Attenuates Ischemia/Reperfusion-Induced Hippocampal Neurons Injury Via Akt-nNOS-JNK Signaling Pathway.* Cell Mol Neurobiol, 2017. **37**(4): p. 753-762.
90. Shvedova, M., et al., *c-Jun N-Terminal Kinases (JNKs) in Myocardial and Cerebral Ischemia/Reperfusion Injury.* Front Pharmacol, 2018. **9**: p. 715.

Figures

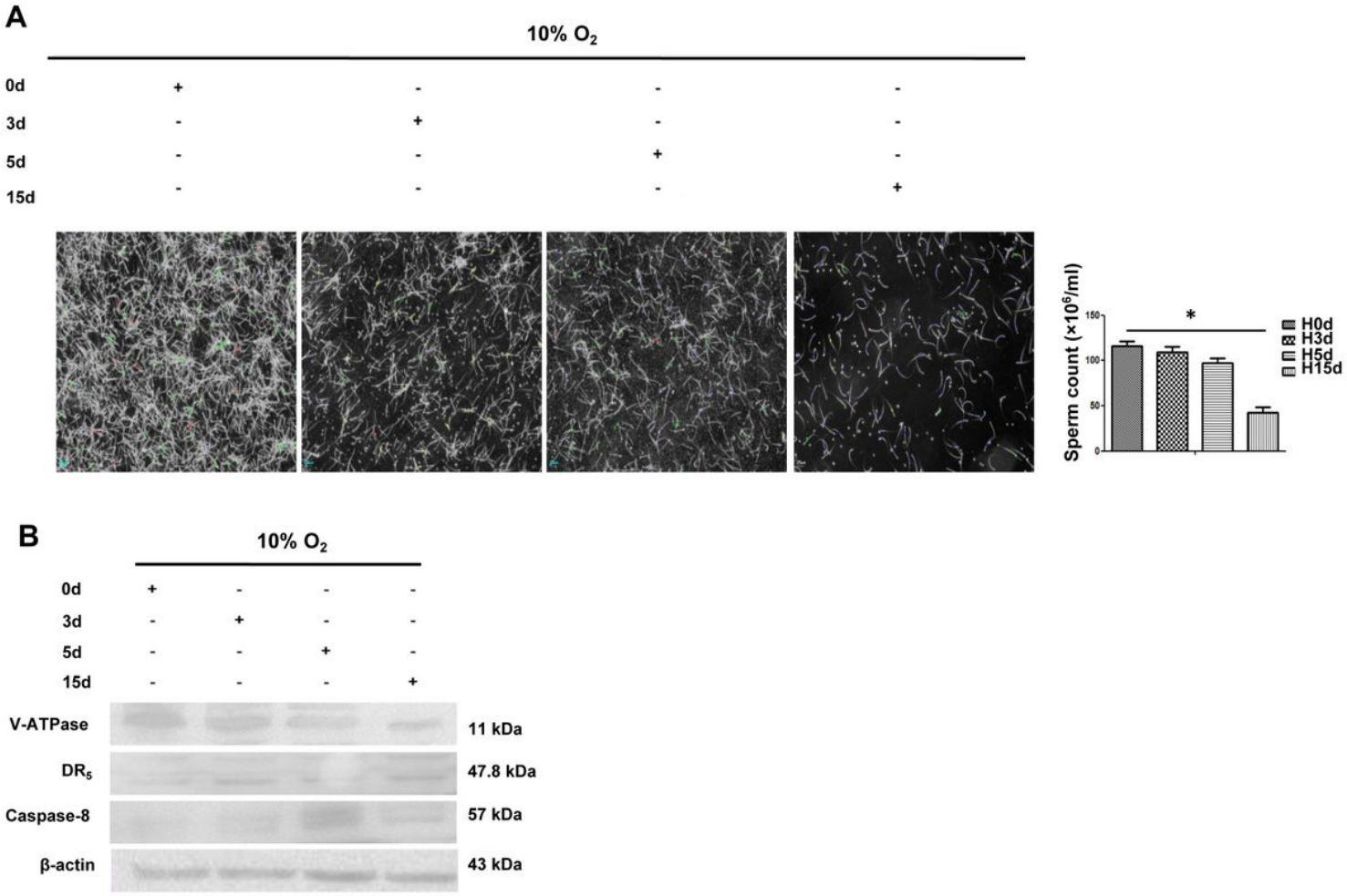

Figure 1

Hypoxia inhibits spermatogenesis and V-ATPase in mice at different times. Hypoxic mice were raised in a hypobaric chamber for 0, 3, 5 or 15 d under 10% O2 condition. (A) Analyses of epididymal sperm collected from hypoxia-treated mice showing total sperm count. (B) Representative western blot assays for V-ATPase, DR5 and caspase-8 protein expression in mouse testis. Data shown are representative of at least three independent experiments.*p< 0.05 vs.control.

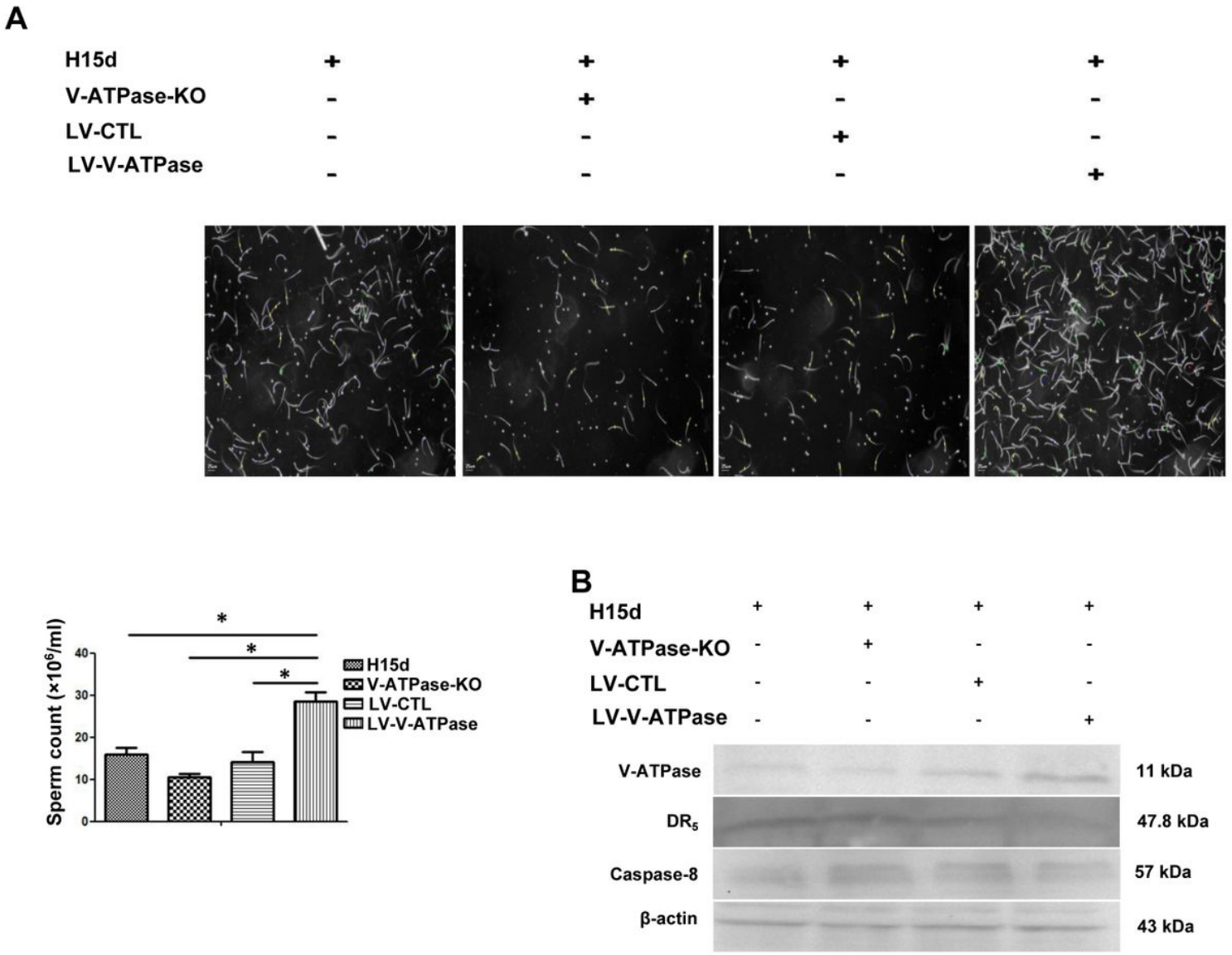

Figure 2

V-ATPase overexpression ameliorates hypoxia-induced spermatogenesis reduction. Hypoxic mice were raised in a hypobaric chamber for 15 dunder 10% O2 condition after injection of LV-V-ATPase. (A) Analyses of epididymal sperm collected from hypoxia-treated mice showing total sperm count. (B)Representative western blot assays for V-ATPase, DR5 and caspase-8 protein expression in mouse testis. Data shown are representative of at least three independent experiments.*p< 0.05 vs.control.

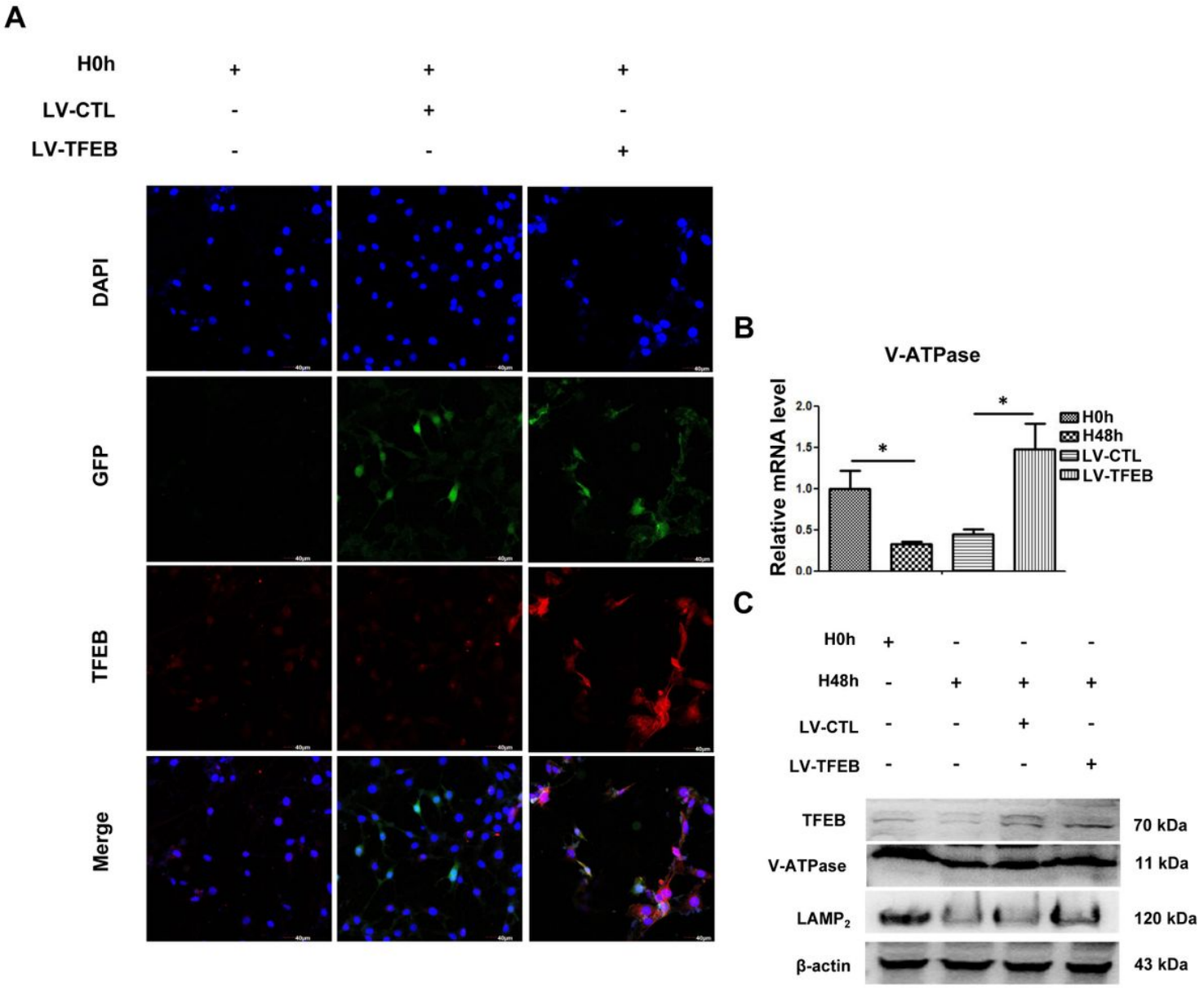

Figure 3

TFEB overexpression normalizes the expression levels of lysosome-related markers under hypoxia treatment in GC-2 cells. GC-2 cells were seeded at 5×105/ml for 48 h in normoxic or hypoxic cultures. GC-2 cells were transfected with LV- TFEB under 1% O2 conditions for 48 h. (A) The colocalization of TFEB expression in nuclei of GC-2 cells from 48h after hypoxia treatment. Representative images show the colocalization of TFEB (red) and DAPI (blue) in GC-2 cells. Scalebar: 40 μm. (B) mRNA levels of V-ATPase and LAMP2 were detected by qPCR in GC-2 cells. The values from treated cells have been normalized to β-actin measurement and then expressed as a ratio of normalized values to mRNA in control cells (n=4). $p<0.05$ vs.control. (C) Representative Western blot assays for V-ATPase and LAMP2 protein expression in GC-2 cells.

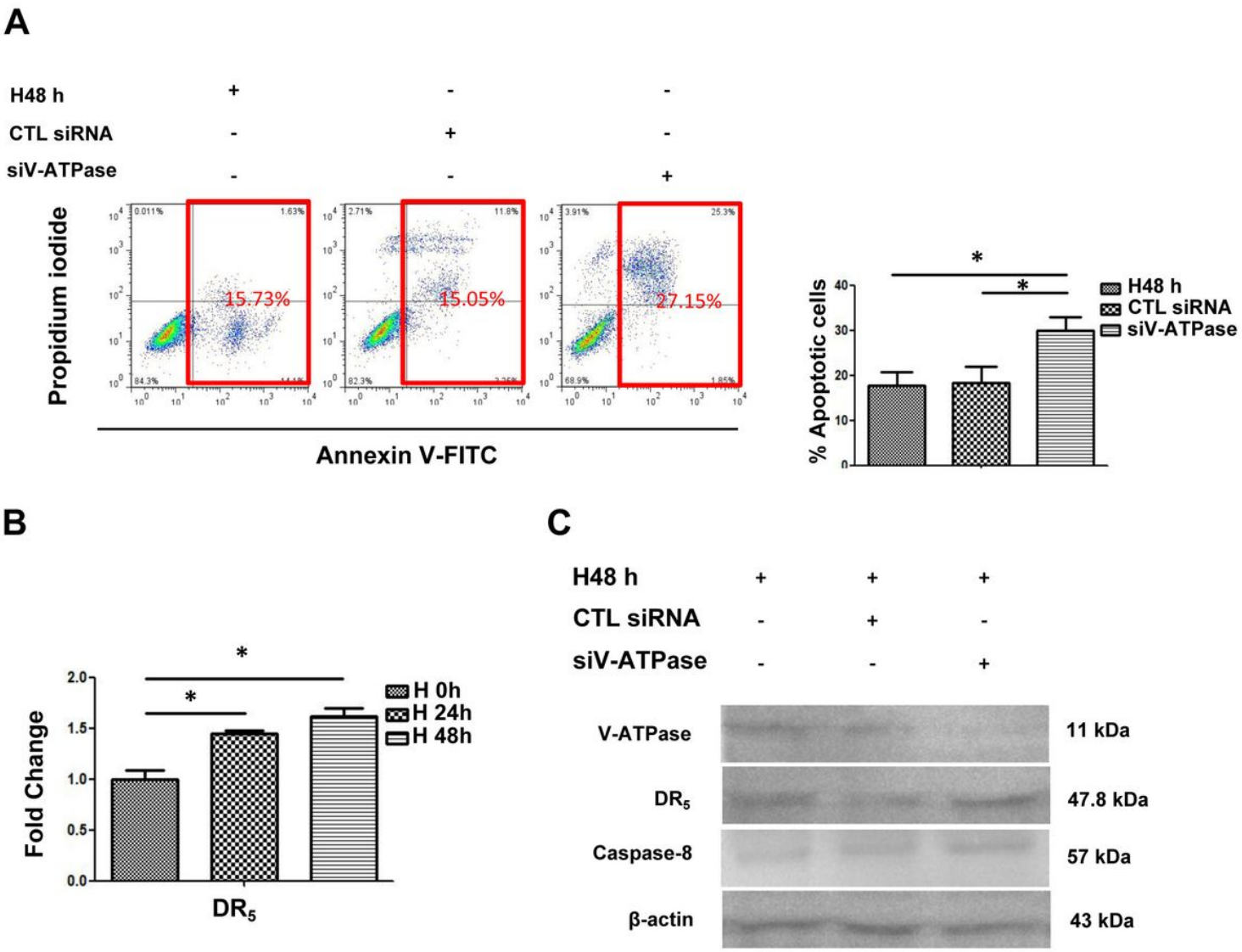

Figure 4

V-ATPase deficiency aggravated hypoxia-induced GC-2 cells apoptosis. GC-2 cells were seeded at5×105/mlfor 48 h in hypoxic culture. V-ATPase deficient GC-2 cells were subjected to 1% oxygen conditions for 48 h.(A) Representative graphs obtained from the flow cytometry analysis of cellular apoptosis afterdouble staining with annexin V-FITC and propidium iodide.(B)The mRNA expression of DR5 by RT-PCR in mouse GC-2 cells. The values from treated cells have been normalized to β-actin measurement and then expressed as a ratio of normalized values to mRNA in control cells (n=4). $p<0.05$ vs.control.(C) The representative western blot assaysfor DR5 and caspase-8protein expression in mouse GC-2 cells that were subjected to 1% oxygen for 48h.

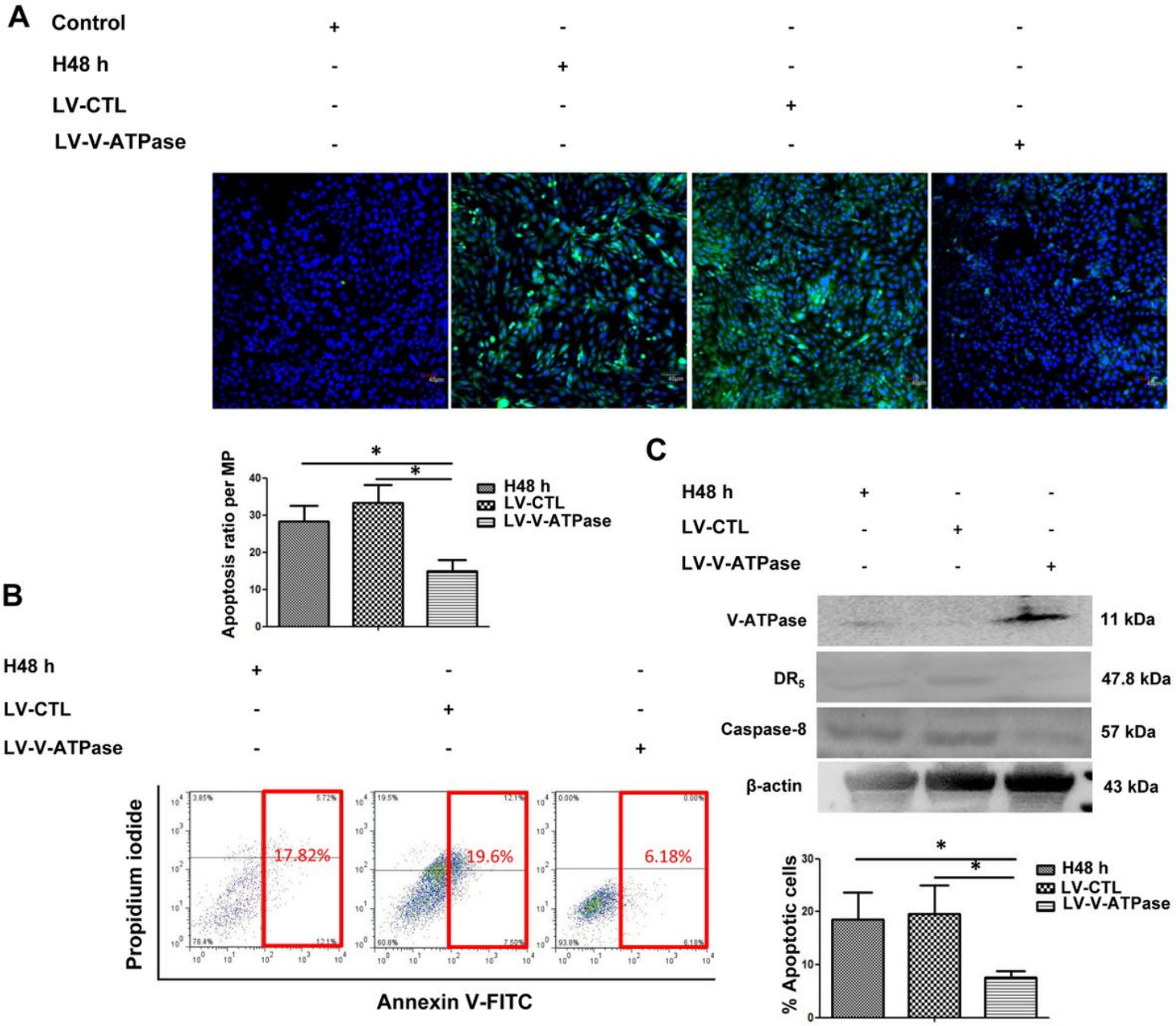

Figure 5

Overexpression of V-ATPase attenuates hypoxia-induced GC-2 cells apoptosis. GC-2 cells were seeded at5×105/ml for48 h in hypoxic culture.GC-2 cellswere transfected with a V-ATPase expression plasmid under 1% O2 conditions 48 h.(A) The TUNEL staining resultsof GC-2 cells: apoptotic nuclei were featured by condensed or fragmented DNA that wasbrightly stained with TUNEL. Original magnification:200×.(B) Representative graphs obtained from the flow cytometry analysis of cellular apoptosis afterdouble staining with annexin V-FITC and propidium iodide. Apoptotic incidences of GC-2 cells were measured by double staining with annexin V-FITC and propidium iodide. (C) The representative western blot assays for V-ATPase, DR5 and caspase-8 protein expression in mouse GC-2 cells that were subjected to 1% oxygen for 48 h.

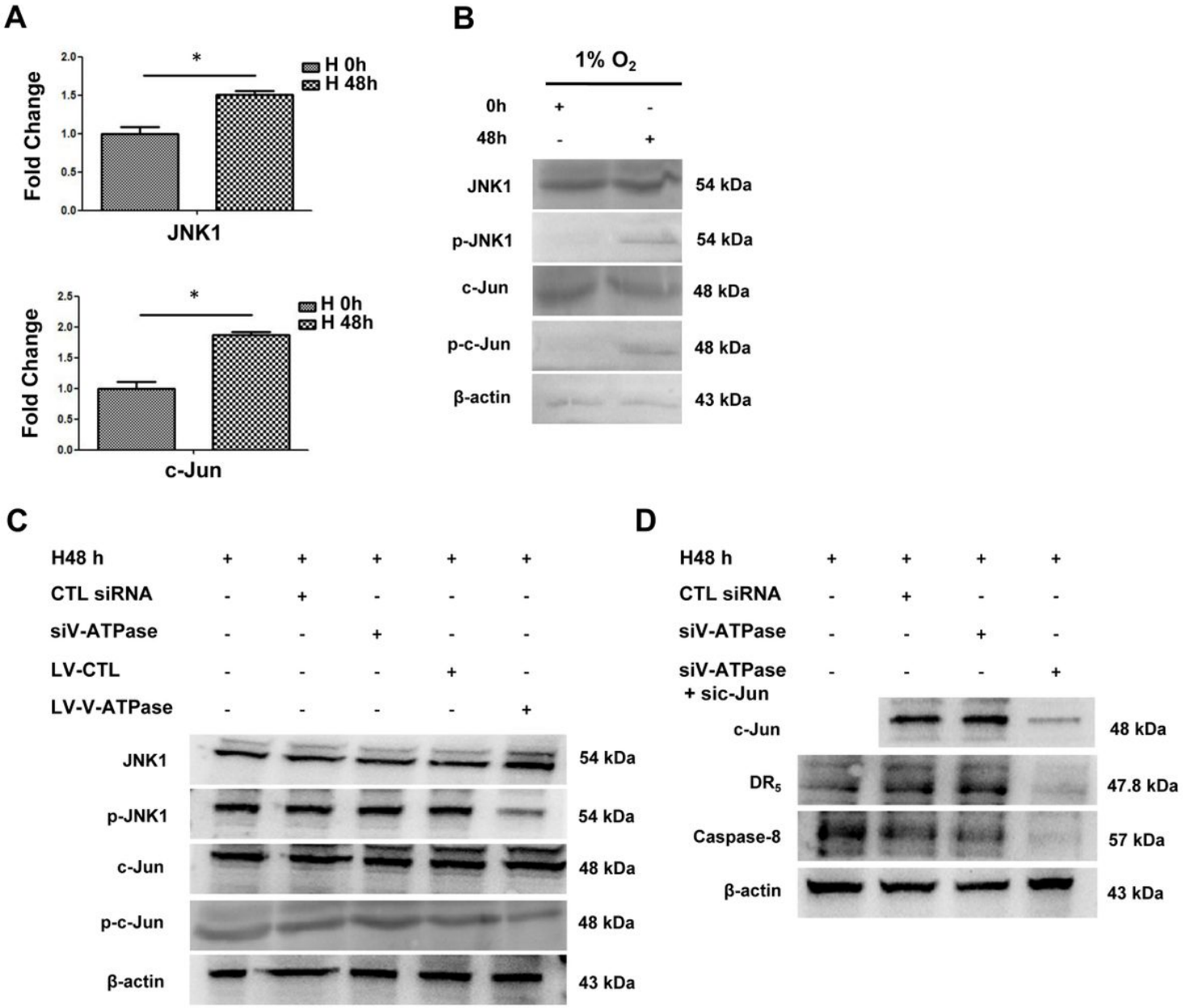

Figure 6

Hypoxia-induced V-ATPase deficiency triggered enhanced apoptosis of GC-2 cells by activating JNK/c-Jun pathway. GC-2 cells were seeded at5×105/ml for48 h in normoxic or hypoxic culture. V-ATPase deficientGC-2 cells were transfected with c-Jun siRNA under 1% O2 condition for 48 h. (A)The mRNA expression of JNK and c-Jun by RT-PCR in mouse GC-2 cells that were subjected to 1% oxygen for 48 h. The values from treated cells have been normalized to β-actin measurement and then expressed as a ratio of normalized values to mRNA in control cells (n=4).p<0.05 vs.control.(B)The representative western blot assays for JNK, c-Jun, p-JNK and p-c-Jun protein expression in mouse GC-2 cells that were subjected to 1% oxygen for 48 h. (C) The representative western blot assays for JNK, c-Jun, p-JNK and p-c-Jun protein expression in V-ATPase deficient or overexpressed GC-2 cells that were subjected to 1% oxygen for 48 h. (D) The representative western blot assays for p-c-Jun, DR5 and caspase-8 protein expression in V-ATPase deficient GC-2 cells transfected with c-Jun siRNA under 1% O2 condition for 48 h.

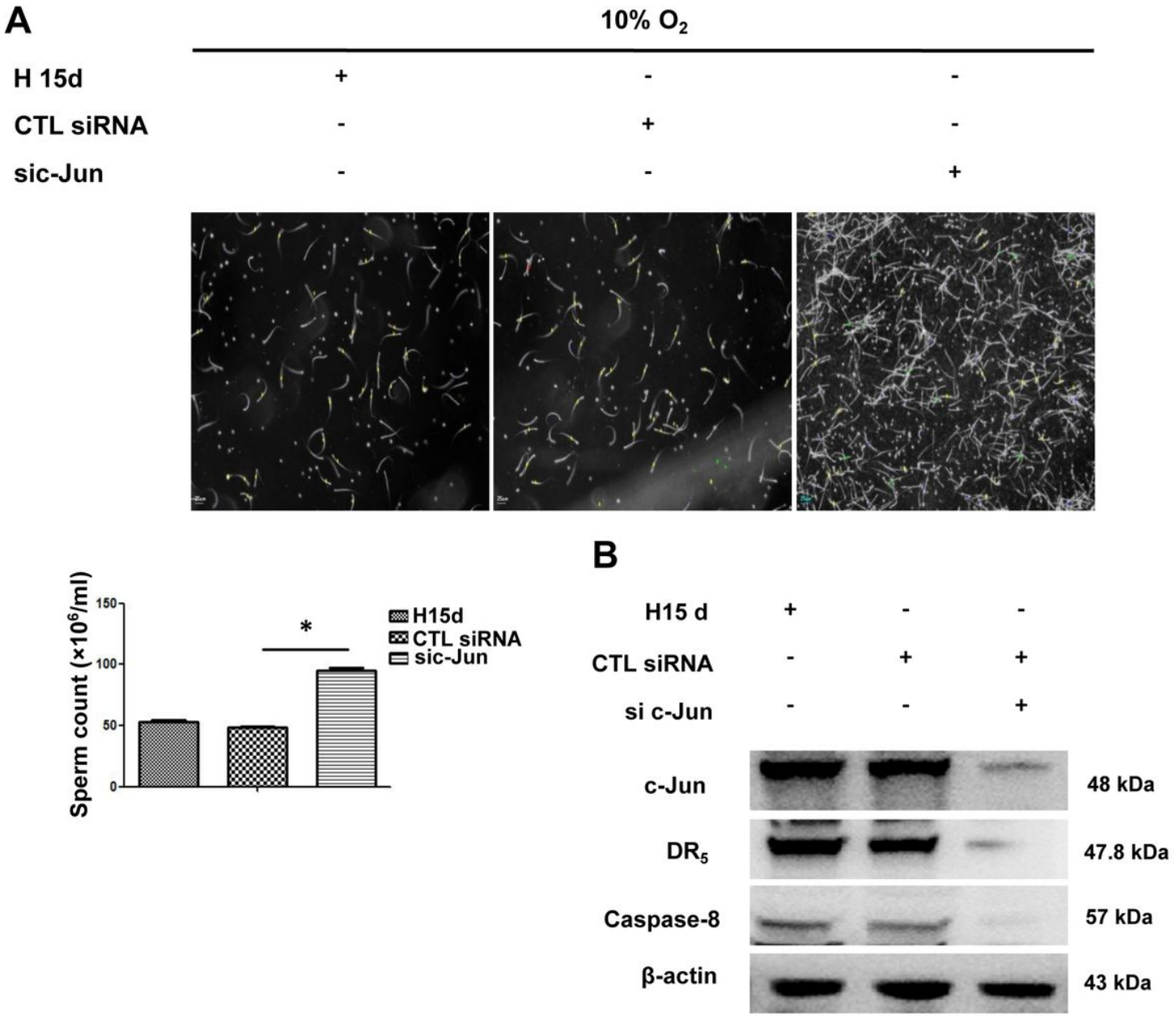

Figure 7

c-Jun deficiency rescues hypoxia-induced spermatogenesis reduction. Hypoxic mice transfected with c-Jun siRNA were raised in a hypobaric chamber for 15 days under 10% oxygen condition. (A) Analyses of epididymal sperm collected from hypoxia-treated mice showing total sperm count. Data shown are representative of at least three independent experiments.*p< 0.05 vs.control. (B) Representative western blot assays for DR5 and caspase-8 protein expression in mouse testis.

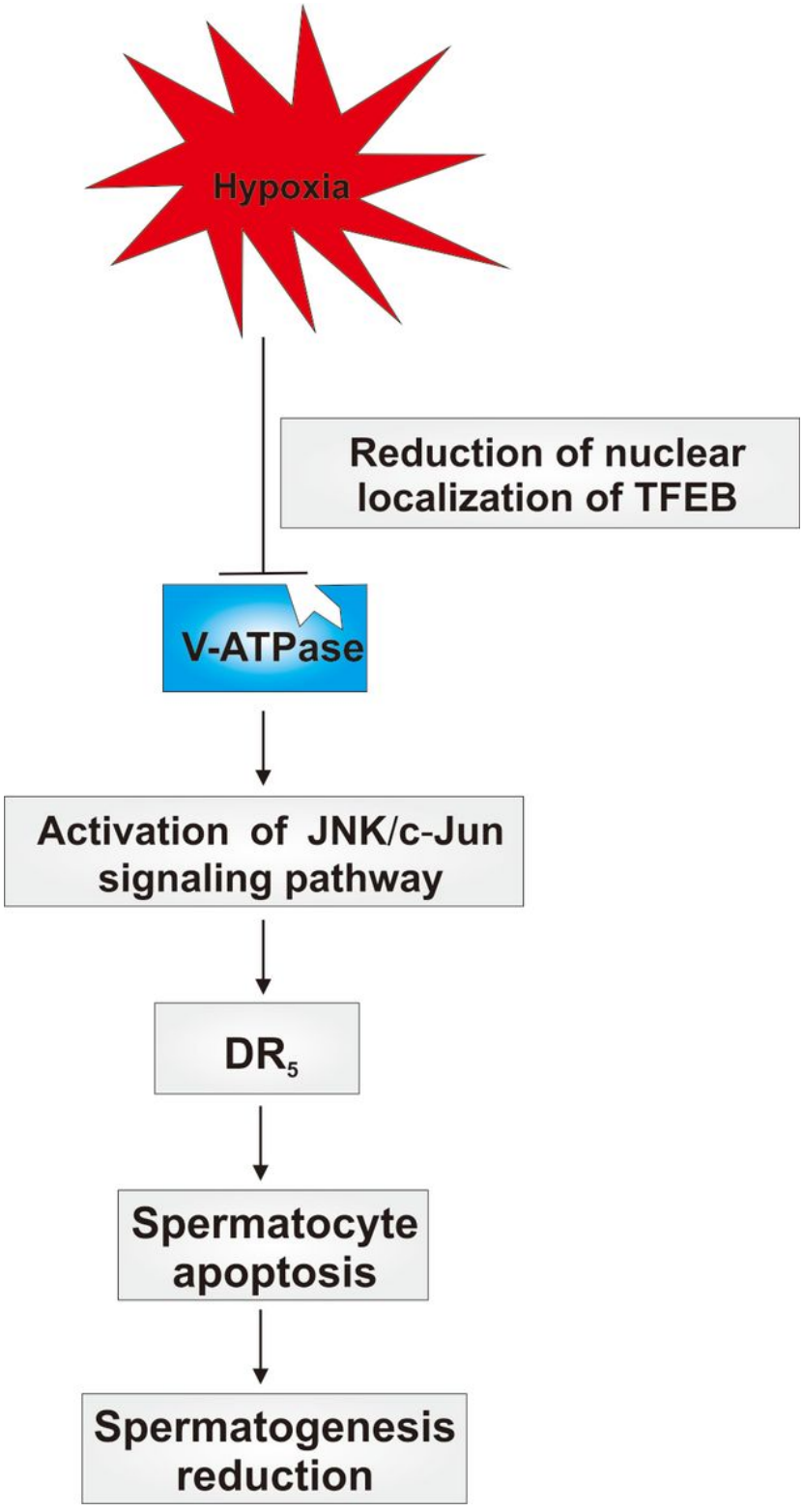

Figure 8

Model for the proposed effects of decreased vacuolar V-ATPase activity. Lower V-ATPase induced by sustain hypoxia presumably leads to activation of DR5 via its transcript factor JNK/c-Jun. Downstream is biological processes important for cellular apoptosis in the spermatocytes. The contribution of spermatocyte apoptosis is prominent spermatogenesis reduction.

Supplementary Files

This is a list of supplementary files associated with this preprint. Click to download.

- FigureS1.jpg
- FigureS2.jpg
- FigureS3.jpg
- FigureS4.jpg
- FigureS5.jpg
- FigureS6.jpg